Polarization and angular dependence of the $L_{2,3}$ absorption edges in Ni(110)

Jan Vogel
Laboratoire pour l'Utilisation du Rayonnement Electromagnétique, bâtiment 209D, Centre Universitaire Paris-Sud, 91405 Orsay, France and Spectroscopy of Solids and Surfaces, University of Nijmegen, Toernooiveld, 6525 ED Nijmegen, The Netherlands

Maurizio Sacchi
Laboratoire pour l'Utilisation du Rayonnement Electromagnétique, Bâtiment 209D, Centre Universitaire Paris-Sud, 91405 Orsay, France
(Received 20 April 1993; revised manuscript received 13 September 1993)

We have measured magnetic circular x-ray dichroism (MCXD) in a remanently magnetized Ni(110) single crystal, with the light in grazing incidence. Measuring the x-ray absorption as a function of the applied magnetic field, we could draw a hysteresis curve similar to one obtained with a magneto-optical Kerr effect on the same crystal. Spectra taken with linearly polarized light show clear variations as the angle of incidence of the light on the sample is changed. The possible origins for this angular-dependent absorption and its consequences for MCXD measurements taken in grazing incidence are discussed.

I. INTRODUCTION

The circularly polarized light which is emitted by synchrotron-radiation sources above and below the plane of the storage ring finds an increasing number of applications. One of the most promising of them is magnetic circular x-ray dichroism (MCXD), i.e., the dependence of the absorption spectra on the helicity of the incoming photons with respect to the magnetization direction in the probed material. In the hard-x-ray range (>3 keV) several experiments have already been done on transition-metal K edges and the L edges of rare earths.[1-3] The exploitation of circularly polarized light in the soft x-ray range (100–2000 eV) is more recent and most of the MCXD results have appeared in the literature during the last three years.[4-10]

Early MCXD experiments in the soft-X-ray range have been done by Chen *et al.*[4] on the L_2 and L_3 absorption edges of a ferromagnetic Ni(111) single crystal. The total absorption spectrum, including the satellite at 6 eV from the main peak, could be reproduced very well using relativistic tight-binding band-structure calculations.[11] To explain the shoulder in the MCXD, however, many-body effects had to be taken into account.[12-14] For other materials, like Fe, the observed MCXD spectra are not yet understood in detail,[15] which has not prevented the development of very interesting practical applications, like the imaging of magnetic domains.[16]

A very important recent development has been the derivation of sum rules for the MCXD, which relate the intensities of the measured spectra and their difference to the spin and orbital magnetic moments in the ground state.[17-19] To apply these rules, however, one needs knowledge of the partial contributions of different transitions to each absorption edge. For the $L_{2,3}$ edges of the $3d$ transition metals, for instance, the polarization-dependent $2p$-$3d$ absorption is superimposed on a background of $2p$-ns transitions, which is not accurately known. Also, other effects can influence the experimentally determined values for the magnetic moments; in this paper we will show that the absorption spectra depend on the angle of incidence of the x rays, especially at angles above 60°. This is of particular importance when data taken at different measuring geometries are compared. We will discuss the different origins which may lead to this angular-dependent absorption, and show another possible use of MCXD, namely to take element-specific hysteresis curves.

II. EXPERIMENTAL DETAILS

The sample we used was a Ni(110) single crystal of $10\times5\times1$ mm, the longer side being along the $[1\bar{1}1]$ direction. After mechanical polishing using diamond grains down to 0.25 μm, the crystal was annealed for 12 h at 650 °C in a 5×10^{-4} mbar hydrogen flow to remove contaminants (mainly sulphur) from the bulk. Final Auger measurements confirmed that the S contamination was below the detectable limit ($<1\%$ of a monolayer). The crystal was mounted on a soft iron horseshoe magnet in a home-built sample holder. In addition to the translation movements, the sample could be rotated around the z axis with a precision of about 0.5° (Fig. 1).

Using the horseshoe magnet, a magnetic field could be applied along the $[1\bar{1}1]$ direction, which is one of the

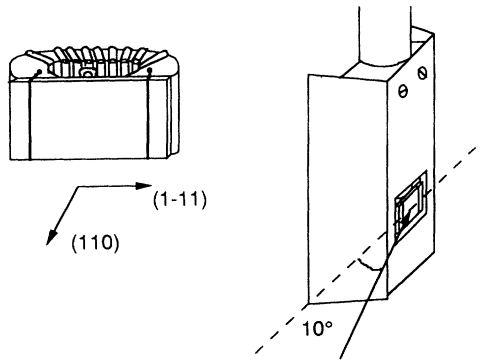

FIG. 1. Mounting of the sample and measuring geometry.

easy magnetization axes of Ni in the (110) plane. From *ex situ* measurements, the intensity of the field was estimated to be about 100 G/A of current in the coils around the magnet. For magnetizing the sample, we could use supplies for pulsed current (up to 40 A) or continuous current (up to 10 A).

The sample was introduced into a ultra-high-vacuum chamber (base pressure 2×10^{-10} mbar) where it could be cleaned using a differentially pumped ion gun and heated by electron bombardment from the back side. Cycles of Ar bombardment and annealing at 800 °C were used to obtain a correct recrystallization of the surface with the corresponding low-energy-electron-diffraction pattern.

X-ray-absorption measurements at the $L_{2,3}$ edges (850–870 eV) were performed on the beamline SA22 of the 800 MeV positron storage ring Super-ACO at Lure (Orsay). The synchrotron light coming from a bending magnet was selected in energy using a UHV double-crystal monochromator. The beryl $(10\bar{1}0)$ crystals used for this experiment give an overall instrumental energy resolution of about 0.3 eV at the nickel edge, as estimated from measurements of the K edge of neon in the gas phase [total (FWHM) ~0.53 eV].

The circularly polarized light we used for our experiments was obtained using high-precision vertical slits, at a distance of 8 m from the source, to select an angular section of 60 μrad at an angle of 1 mrad below the orbit plane. In these conditions the light is elliptically polarized with negative helicity and the degree of circular polarization ξ_2 is about 0.9. Monochromatizing at ~850 eV with beryl crystals implies two Bragg reflections close to 67°, reducing ξ_2 to about 0.55 at the sample position.[6]

Spectra of the $L_{2,3}$ edges of Ni were collected both in total electron yield mode (TEY) using a channeltron with a positive bias of 100 V on the front end, and in current mode using an interfaced picoamperometer. The results obtained in both ways were equivalent, but TEY gave a better signal-to-noise ratio. Consequently, the data reported here have all been obtained in TEY.

III. RESULTS

A. Circularly polarized light

In Fig. 2, the Ni $L_{2,3}$ edges are shown measured with the light emitted 1 mrad below the plane. The light was incident 10° off the $[1\bar{1}1]$ magnetization axis of the crystal (see Fig. 1). Open and closed circles correspond to opposite signs of the current in the electromagnet, i.e., to opposite magnetizations along the $[1\bar{1}1]$ axis. The spectra were taken with the crystal remanently magnetized, after a current pulse of 40 A. The sum of the peak heights of the L_3 is set to 100. The difference curve in Fig. 3 is corrected both for the incomplete polarization of the light ($\xi_2=0.55$ at 850 eV) and for the fact that ξ_2 is not constant over the measured energy range (it is about a factor of 1.2 smaller at the L_2 than at the L_3 edge[20]). We have not corrected for the disalignment of 10° between the light-propagation vector and the magnetization axis.

We used the spectra from Fig. 2 to obtain the L_3:L_2

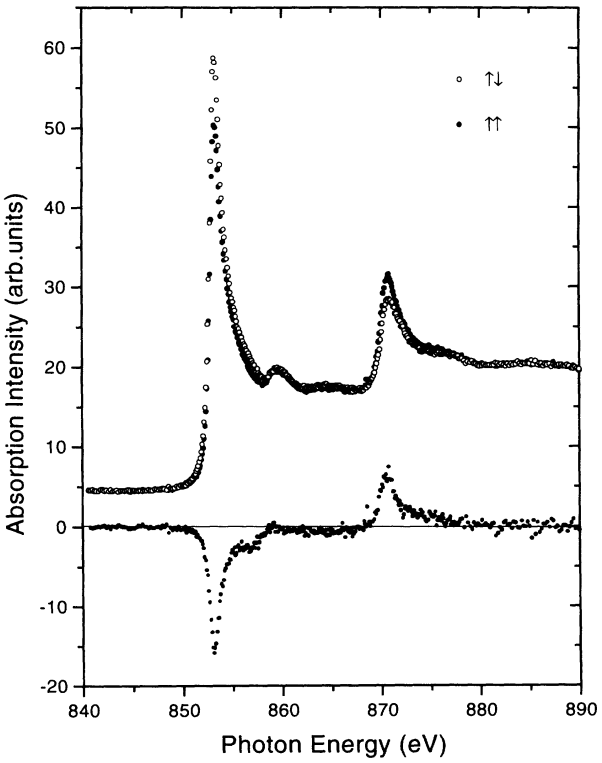

FIG. 2. Spectra taken below plane ($\varphi=1$ mrad) with helicity of the light and Ni majority-spin direction parallel (●) and antiparallel (○), together with the difference curve.

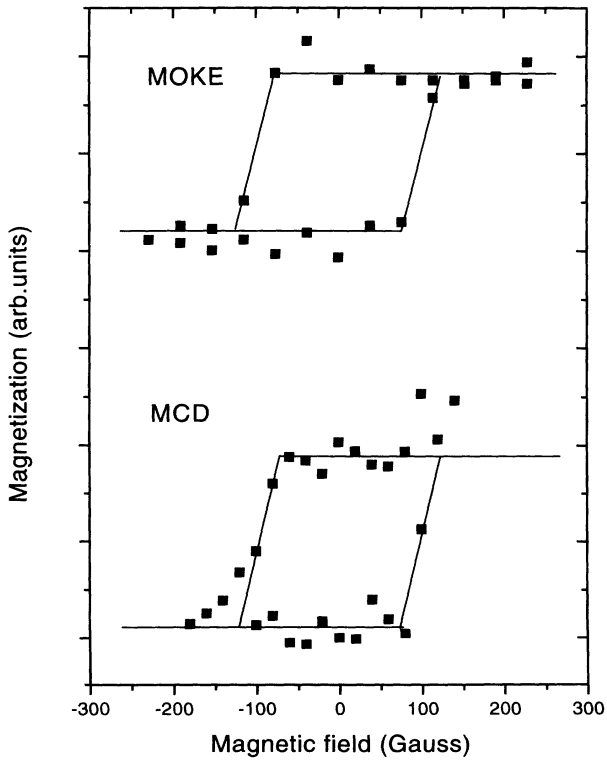

FIG. 3. Hysteresis curves taken with MOKE (top) and MCXD (bottom) on Ni(110). The drawn lines are guides to the eye.

branching ratios of the total spectrum ($\sigma_+ + \sigma_-$) and of the difference curve ($\sigma_+ - \sigma_-$), and the asymmetry at the maximum of the L_3. Using the above-mentioned sum rules, we derived the expectation values of the orbital and spin moments of the d shell $\langle L_z \rangle$, $\langle S_z \rangle$ and the total momentum $\langle L_z \rangle + 2\langle S_z \rangle$ from our spectra. In Table I, they are compared with the ones from the experiments of Chen *et al.*[4] The values they obtained for $\langle L_z \rangle$ and $\langle S_z \rangle$ from comparison of their data with tight-binding calculations[11] are identical to those found by Thole *et al.*[17,18] using the sum rules. As in our case, their Ni single crystal was magnetized along a [111] direction, but perpendicular to the surface plane, and the spectra were measured with the x rays at normal incidence. The parameters for the two geometries are remarkably close, considering the angular dependence of the absorption spectra discussed below.

We also measured the absorption curve with a continuous current flowing through the wires of the horseshoe magnet. We found stable and reproducible data up to about 2 A, indicating a fairly well-closed magnetic circuit with very small stray fields. For higher currents, the signal-to-noise ratio degraded rapidly.

In order to draw semiquantitative conclusions from the current dependence of the x-ray-absorption spectroscopy (XAS) spectra we adopted the following procedure: (i) a reference spectrum (S_{ref}) was taken after a negative current pulse; (ii) after normalization of the spectra, S_{ref} was subtracted from each spectrum $S(I)$ measured with a continuous current flow I; (iii) the difference was integrated over the energy range 850–860 eV (L_3 edge) to give the area $A(I)$ as a function of the current I.

The resulting values of $A(I)$ are plotted in Fig. 3 for I ranging from -2 to $+2$ A. The hysteresis curve taken with MCXD shows that the Ni crystal we used exhibits a remanence at zero field of 100%, in agreement with a magneto-optical Kerr effect (MOKE) measurement performed on the same sample and the same mounting, before inserting the manipulator in the vacuum chamber.

B. Linearly polarized light

In Fig. 4 we present some experimental data obtained in-plane (linearly polarized light) by changing the angle of incidence of the photons on the sample. Shown are three spectra taken at $\alpha = 0°$ (normal incidence), 60°, and 75°, which present clear changes in the relative height of the structures. In Table II we give the normalized L_3 and L_2 peak heights for different angles of incidence, together with the total integrated intensity (normalized to 100 for normal incidence) and the L_3:L_2 branching ratio. To determine the intensities and branching ratios, we normalized the experimental spectra at two points, before the L_3 edge and after the L_2 edge. An extra check of the validity of this procedure consists of the fact that normalized in this way, the intensities in between the L_3 and L_2 edges coincide. After normalization, we subtracted a double-step function (also shown in Fig. 4), with the first step at the maximum of the L_3 and the second of half height shifted of the spin-orbit term of the $2p$ core hole ($\xi = 17.3$ eV). Although it is quite rough, this is a gen-

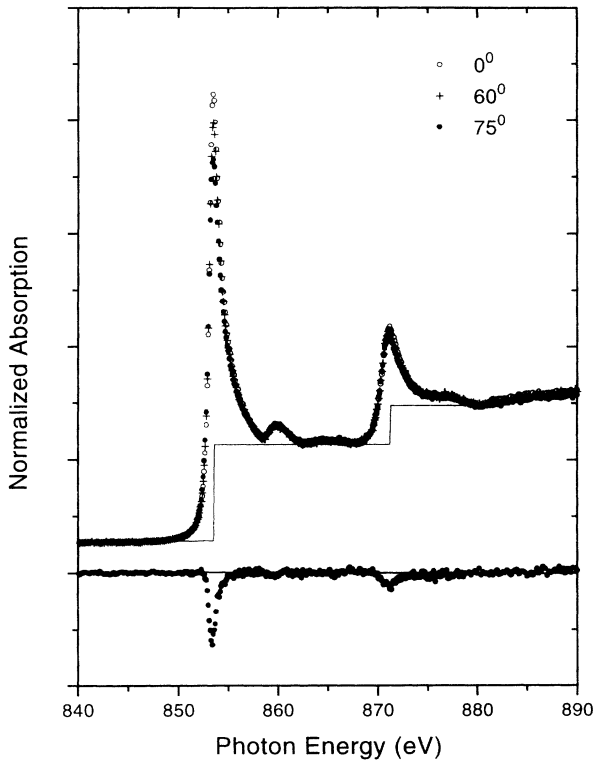

FIG. 4. Spectra taken in plane ($\varphi = 0$ mrad) for normal (○), 60° (+), and 75° incidence (●), together with the difference between the normal and 75° incidence spectra.

TABLE I. The experimental parameters obtained from our spectra compared to those of Chen *et al.* (Refs. 4, 11, 17, 18).

	Chen *et al.*	This work
L_3/L_2 (tot.)	2.6	2.6±0.2
L_3/L_2 (diff.)	−1.6	−1.7±0.2
$\langle L_z \rangle (\mu_B)$	0.05	0.06±0.01
$\langle S_z \rangle (\mu_B)$	0.26	0.27±0.03
$\langle L_z \rangle + 2\langle S_z \rangle (\mu_B)$	0.57	0.60±0.05

TABLE II. Normalized L_3 and L_2 peak heights, total integrated intensities, and branching ratios for different angles of incidence. The error bar on the branching ratios is estimated to be about 0.2.

Angle	L_3 max.	L_2 max.	Integrated L_3+L_2	Branching ratio
0	100.0	51.1	100.0	2.7
10	103.3	50.8	102.0	2.8
20	103.2	50.7	100.3	2.8
30	100.1	50.9	98.7	2.7
40	99.1	50.0	97.7	2.7
50	98.2	50.6	98.5	2.7
60	93.9	49.9	96.9	2.6
70	91.7	50.2	94.8	2.7
75	86.1	48.9	91.7	2.8
80	83.7	48.2	90.0	2.6

erally accepted way to determine branching ratios of transition-metal $L_{2,3}$ edges.

The most likely explanation for the lowering of the peaks going to grazing incidence consists of angular-dependent saturation, as already reported for absorption and photoemission from the $3d$ core states in rare earths.[21,22] According to Thole *et al.*,[23] a simple model for x-ray absorption in TEY gives

$$Y = A\int_0^\infty e^{-x/[\lambda(\omega)\cos\theta]}dx/[\lambda(\omega)\cos\theta]e^{-x/d} = Ad/[d+\lambda(\omega)\cos\theta],$$

where Y is the total yield, A is the number of electrons produced per photon, which run in the direction of the surface, θ is the angle of incidence of the x rays, $\lambda(\omega)$ is the absorption length at energy ω, and d is the probing depth of TEY. For $d \ll \lambda(\omega)\cos\theta$ this is approximately equal to $(Ad)/\lambda(\omega)\cos\theta$, making the measured yield inversely proportional to the absorption length and thus, proportional to the absorption coefficient. For smaller $\lambda(\omega)\cos\theta$, i.e., for higher θ and/or at the maximum of the absorption [where $\lambda(\omega)$ is the smallest], saturation can occur.

In Fig. 5 the normalized L_3 peak heights are plotted, taken from Table II. Supposing that before and after the edges, the condition $d \ll \lambda(\omega)$ is fulfilled and thus, $Y = (Ad)/\lambda(\omega)\cos\theta$, normalizing the spectra there means

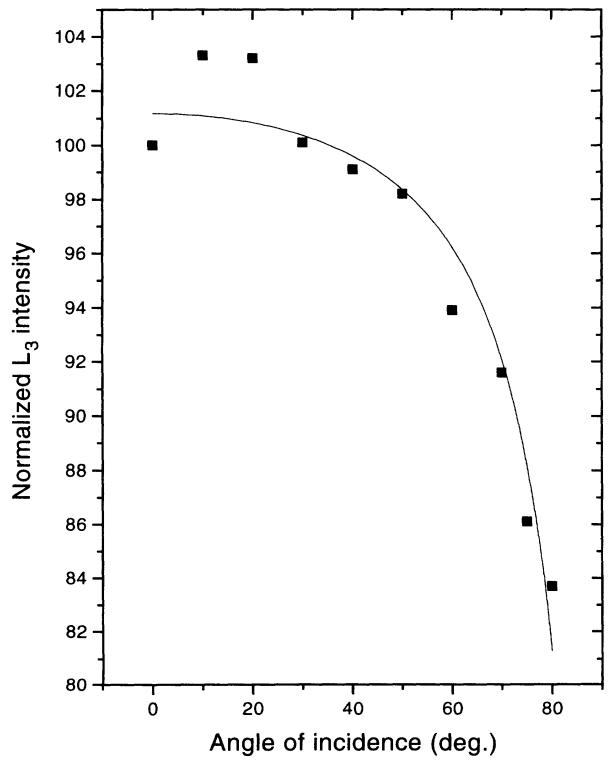

FIG. 5. Normalized L_3 peak heights for different angles of incidence, taken from Table II. The drawn line is a fit with a function $F(\theta) = A\cos\theta/(1+k\cos\theta)$, with $k = \lambda/d = 18\pm2$ (see text).

putting the yields Y equal for different angles or, equivalently, multiplying the measured spectra with $\cos\theta$. To fit the intensities at the edges we used, therefore, a function $F(\theta) = A\cos\theta/(1+k\cos\theta)$, where $k = \lambda/d$. The result of the fit is also shown in Fig. 5, giving a value of $k = 18\pm2$. A similar fit for the L_2 peak height gave a value of $k = 80\pm10$. In Table II also, the total integrated intensities, obtained after subtracting the step function, are given. The decrease of the intensities starts to get important at angles of incidence higher than 60°, going from less than 3% at 60° to about 10% at 80°.

Although the function $F(\theta)$ gives good fits for all the experimental data, other observations, like the occurrence of analogous (though smaller) effects in 1–5 monolayer (ML) thin layers of Ni on Fe,[24] suggest that other effects may also play a role. Two of them we give below.

(i) Like visible light, x rays are partly reflected going from one medium to another. The reflectivity R is, in general, very small and starts getting important only for angles of incidence close to 90°. However, near absorption edges of high cross section, the reflectivity may be non-negligible at much lower angles. This effect has been clearly measured in NiO and TbFe samples,[25] showing the existence of large variations in R and, consequently, in the absorption already at angles of 80°; (ii) an alternative and more appealing interpretation calls for the existence of linear magnetic dichroism in metallic nickel. It would originate both from the bulk, where the effect is caused by the anisotropy of the charge distribution ($\langle M^2 \rangle$), and from the surface, where the magnetic moment is expected to be larger than in the bulk.[26,27] Also, the surface itself gives rise to an anisotropic charge distribution, due to electrostatic effects. The linear dichroism from the bulk, as expected from an Anderson impurity model, looks more or less like the circular dichroism, but with all peaks having the same sign.[28] Preliminary results that we obtained on our Ni(110) crystal after rotating it 90° azimuthally (and so changing the relative orientation of the polarization vector of the light and the magnetization axis without changing the incidence angle of the x rays) suggest that this effect is very small, but, nevertheless, deserves further investigation.

IV. SUMMARY AND CONCLUSIONS

In this paper we have presented results of angular- and polarization-dependent x-ray absorption in a Ni single crystal. The main conclusions of this work are (i) the magnetic parameters obtained from the MCXD at grazing incidence compare very well with reference data taken at normal incidence, even though the absolute intensities of the peaks change considerably. Apparently, the different integrated intensities needed to calculate $\langle L_z \rangle$ and $\langle S_z \rangle$ with the sum rules of Thole *et al.* are influenced in a similar way. This is of interest for measuring materials which have their easy axis of magnetization in the surface plane, like many magnetic multilayers; (ii) the intensities obtained from the spectra as a function of the angle of incidence can be fitted with a function $F(\theta) = A\cos\theta/(1+k\cos\theta)$, supposing satura-

tion effects. For the maximum of the L_3 intensity, we find a value of $k=\lambda/d=18\pm2$. The decrease of the intensities starts getting important above 60°, going from less than 3% to about 10% at 80°. This is of particular importance when one wants to compare spectra taken at different angles on different samples. This was done, for instance, in a recent paper about MCXD in Co/Pd multilayers.[7] The large difference between the peak intensities in a multilayer measured in normal incidence and a pure Co layer measured in grazing incidence that was reported, can certainly not be attributed to angular-dependent effects only, but our data show that they should be taken into account for a more accurate and reliable analysis; (iii) effects other than saturation might contribute to the angular dependence of the absorption spectra. The existence of linear magnetic dichroism in Ni metal [an effect similar to that has already been observed in NiO (Ref. 25) and Fe_2O_3 (Ref. 29)] would, apart from a theoretical point of view, be of particular interest for systems in which different Ni layers are coupled antiferromagnetically, like in some magnetic multilayers, and which, therefore, exhibit no circular dichroism; (iv) Using MCXD, one can obtain hysteresis curves in an element-selective and surface-sensitive way. Recently this was nicely confirmed by measurements on Fe/Cu/Co trilayers.[9] Analogous studies can be performed on surface or buried layers and diluted samples (impurities, etc.).

ACKNOWLEDGMENTS

We thank Gerrit van der Laan for his suggestions and for supplying us with preliminary results of his calculations of linear dichroism in nickel. This work has been supported in part by the Stichting Scheikundig Onderzoek in Nederland (SON) with financial support from the Nederlandse Stichting voor Wetenschappelijk Onderzoek (NWO), and by the European Community under Contract No. SC1-CT91-0630.

[1]G. Schütz, W. Wagner, W. Wilhelm, P. Kienle, R. Zeller, R. Frahm, and G. Materlik, Phys. Rev. Lett. **58**, 737 (1987); G. Schütz, M. Knülle, R. Wienke, W. Wilhelm, W. Wagner, P. Kienle, and R. Frahm, Z. Phys. B **73**, 67 (1988).

[2]F. Baudelet, E. Dartyge, A. Fontaine, C. Brouder, G. Krill, J. P. Kappler, and M. Piecuch, Phys. Rev. B **43**, 5857 (1991).

[3]J. C. Lang, S. W. Kycia, X. D. Wang, B. N. Harmon, A. I. Goldman, D. J. Branagan, R. W. McCallum, and K. D. Finkelstein, Phys. Rev. B **46**, 5298 (1992).

[4]C. T. Chen, F. Sette, Y. Ma, and S. Modesti, Phys. Rev. B **42**, 7262 (1990).

[5]L. H. Tjeng, Y. U. Idzerda, P. Rudolf, F. Sette, and C. T. Chen, J. Magn. Magn. Mater. **109**, 288 (1992); P. Rudolf, F. Sette, L. H. Tjeng, G. Meigs, and C. T. Chen, *ibid.* **109**, 109 (1992).

[6]Ph. Sainctavit, D. Lefebvre, Ch. Cartier, C. Lafon, C. Brouder, G. Krill, J.-Ph. Schillé, J.-P. Kappler, and J. Goulon, J. Appl. Phys. **72**, 1985 (1992).

[7]Y. Wu, J. Stöhr, B. D. Hermsmeier, M. G. Samant, and D. Weller, Phys. Rev. Lett. **69**, 2307 (1992).

[8]J. G. Tobin, G. D. Waddill, and D. P. Pappas, Phys. Rev. Lett. **68**, 3642 (1992).

[9]C. T. Chen, Y. U. Idzerda, H.-J. Lin, G. Meigs, A. Chaiken, G. A. Prinz, and G. H. Ho, Phys. Rev. B **48**, 642 (1993).

[10]Y. U. Idzerda, L. H. Tjeng, H.-J. Lin, C. J. Gutierrez, G. Meigs, and C. T. Chen, Phys. Rev. B **48**, 4144 (1993).

[11]C. T. Chen, N. V. Smith, and F. Sette, Phys. Rev. B **43**, 6785 (1991).

[12]T. Jo and G. A. Sawatzky, Phys. Rev. B **43**, 8771 (1991).

[13]G. van der Laan and B. T. Thole, J. Phys. Condens. Matter **4**, 4181 (1992).

[14]A. Tanaka and T. Jo, J. Phys. Soc. Jpn. **61**, 2669 (1992).

[15]N. V. Smith, C. T. Chen, F. Sette, and L. F. Mattheis, Phys. Rev. B **46**, 1023 (1992).

[16]J. Stöhr, Y. Wu, B. D. Hermsmeier, M. G. Samant, G. R. Harp, S. Koranda, D. Dunham, and B. P. Tonner, Science **259**, 658 (1993).

[17]B. T. Thole, P. Carra, F. Sette, and G. van der Laan, Phys. Rev. Lett. **68**, 1943 (1992).

[18]P. Carra, B. T. Thole, M. Altarelli, and X. Wang, Phys. Rev. Lett. **70**, 694 (1993).

[19]M. Altarelli, Phys. Rev. B **47**, 597 (1993).

[20]Ph. Sainctavit (unpublished).

[21]O. Sakho, M. Sacchi, F. Sirotti, and G. Rossi, Phys. Rev. B **47**, 3797 (1993).

[22]G. van der Laan and B. T. Thole, J. Elecron Spectrosc. Relat. Phenom. **31**, 1 (1983).

[23]B. T. Thole, G. van der Laan, J. C. Fuggle, G. A. Sawatzky, R. C. Karnatak, and J.-M. Esteva, Phys. Rev. B **32**, 5107 (1985).

[24]J. Vogel and M. Sacchi (unpublished).

[25]D. Alders, C. Levelut, J. Vogel, S. Peacor, M. Sacchi, and G. A. Sawatzky (unpublished).

[26]A. J. Freeman and Ru-qian Wu, J. Magn. Magn. Mater. **100**, 497 (1991).

[27]G. van der Laan, M. A. Hoyland, M. Surman, C. F. J. Flipse, and B. T. Thole, Phys. Rev. Lett. **69**, 3827 (1992).

[28]G. van der Laan (private communication).

[29]P. Kuiper, B. G. Searle, P. Rudolf, L. H. Tjeng, and C. T. Chen, Phys. Rev. Lett. **70**, 1549 (1993).